

ATTENUATION ANALYSIS OF VSP DATA

by

Suprajitno Munadi

ABSTRACT

Attenuation is usually defined to include all types of frequency selective process which contribute to the amplitude decay of propagating waves. It depends on porosity of rock, grain size, over pressure zones and fluid saturation. Attenuation can at least double the information obtained from velocities alone.

The measurement of attenuation from a Vertical Seismic Profiles (VSP) has been carried out using two different methods i.e. the Spectral Magnitude Decay Method and the Pulse Broadening Method. The Spectral Magnitude Decay Method is executed in the frequency domain, while the Pulse Broadening Method is entirely executed in the time domain.

Both methods have been tested using two shallow, high resolution VSP data. The deduced quality factor Q , obtained from the Spectral Magnitude Decay Method is slightly lower than those obtained from the Pulse Broadening Method. These discrepancies can be attributed to reflection/transmission losses at layer boundaries which are lumped together with absorption in the frequency domain estimates.

1. INTRODUCTION

Attenuation is an important seismic attribute. It provides diagnostic information on certain rock properties such as degree of fluid saturation (Biot, 1956; Gardner et al., 1964; White, 1975; Mavko and Nur, 1978), over-pressured zones (Gardner et al., 1964; Toksoz et al., 1979), porosity and grain size (Hamilton, 1972). In seismic interpretation, attenuation can at least double the information obtained from velocities alone (Toksoz and Johnston, 1981). In data processing, attenuation estimates are needed for time-variant gain compensation and for improving the resolution of seismic data (deconvolution).

The measurement of attenuation from a VSP survey (Fig. 1) is considered to be the most successful field method. Analysis of anelastic absorption from VSP data have been reported in the literature using the transfer function method (Tullos and Reid, 1969; Spencer et al., 1982; Lee and Balch, 1983) and the spectral ratio method (McDonald et al., 1958; Kudo and Shima, 1970; Hauge, 1981). Both methods are long and tedious and suffer from difficulties in isolating the first arrival transmitted wave. The correct geometrical spreading factors for multilayered media

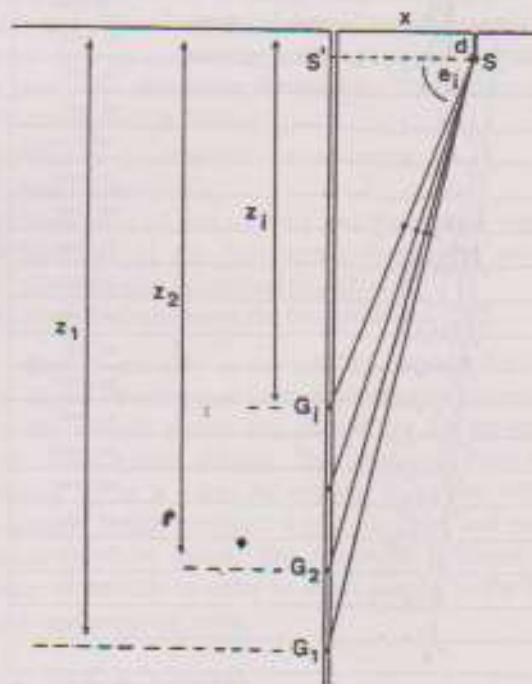


Figure 1 The first arrivals and the slant ray path in conventional offset - VSP shooting.

are also difficult to find. Unless reflection/transmission losses within the layer stack can be removed, the Q value obtained is always an under-estimate.

In this paper, we present an alternative pulse-broadening method for determining attenuation which overcomes most of the above difficulties. We also present a revised spectral magnitude scheme which acts on the primary downgoing wave. This event is isolated in f - k space using the "contour-slice filter method" (see Suprajitno and Greenhalgh 1985).

II. RAW VSP DATA

Figure 2 shows the raw VSP record from borehole W. The record consists of 20 traces spaced at a depth interval of 5 metres. In this display there is no gain compensation applied, but each trace has been normalised to its maximum amplitude, which has been written to the right of the record. The shot-

point was offset 25 metres from the well head, at a depth of 2 metres. There is an instrument problem evident on traces 17 to 20 (upper 4 traces).

Figure 3 shows the VSP records from hole Y. The geophone interval is 10 metres. Trace number 1 (bottom) was a misfire. Traces 2 and 3 were recorded at the deepest level (230m) from shots in a steel cased hole offset 25m from the borehole. Note the consistency of waveforms between the two traces. Casing collapse from subsequent shooting (trace 4) precluded further use of the shot hole. All remaining shots (traces 5 to 20) were fired at 1m depth in a mud pit distant 4m from the borehole. The conspicuous low frequency event at around 220msec which trails and replicates the first arrivals is a bubble-pulse type echo arising from reverberation within the mud pit. Fortunately, it doesn't overlap the primary arrivals and it can be removed by straight velocity windowing and/or frequency filtering.

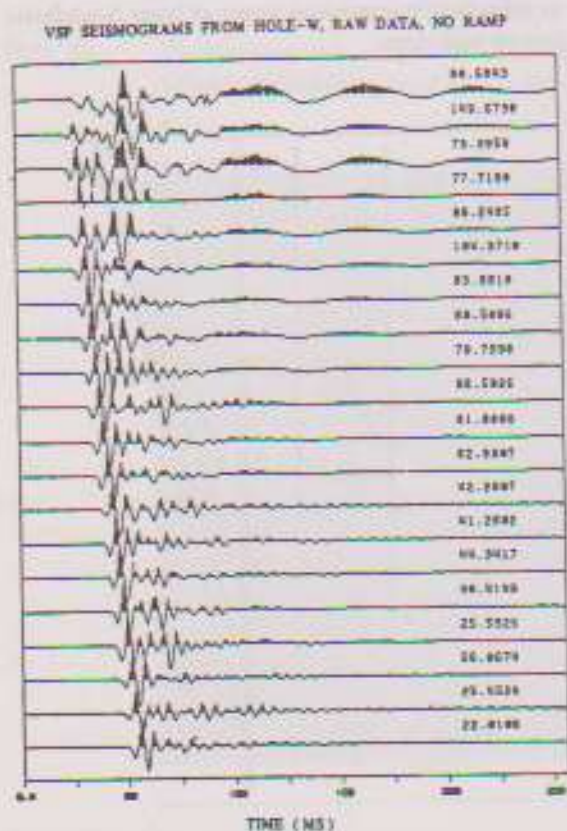


Figure 2 The raw VSP data from hole W, The depth spacing is 5 m.

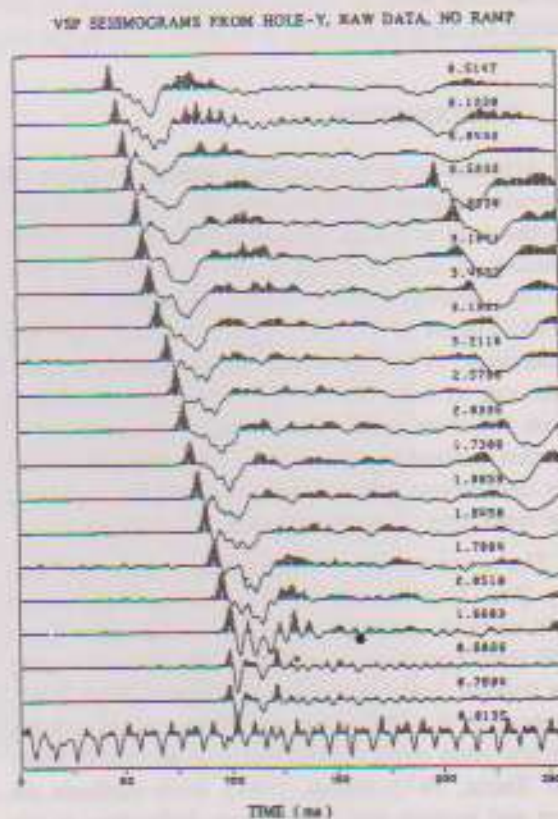


Figure 3 The raw VSP data from hole Y, The depth spacing is 10 m.

III. THE SPECTRAL DISPLAY

The spectral display from a VSP record provides a rough indication of progressive earth filtering effects along the borehole. The changing of spectral shape from successive levels indicates energy losses which signify the absorption and transmission/reflection response of the earth. Such information can be used as an aid in optimizing acquisition and processing parameters.

There are several methods that can be used to compute the spectra of a VSP trace, i.e. Auto correlation method (Blackman and Tukey, 1959), Fast Fourier transform method (Bath, 1974), Moving Average method (Box and Jenkins, 1976), Auto Regressive Moving Average (Treitel et al., 1977; Gutowski et al., 1978), Maximum Entropy method (Burg, 1967) and Maximum Likelihood method (Lacoss, 1971). Each method has its own superiority/inferiority and has been devised to be suitable for an assumed physical process which generates the signal.

For the purpose of spectral display, we will follow Bath (1974,p.179). In this case the VSP trace is windowed first in the time domain before computing its spectra. Then, the fast Fourier transform is used to obtain the spectral magnitude.

A. The Trace Spectra of Hole W

The spectra for hole W, traces 1 to 20, are shown in Figure 4. Again, amplitude normalisation factors for each trace appear to the right hand side of the diagram. The bandwidth extends to a frequency of approximately 300Hz. Broadly speaking, the figure confirms our intuitive expectation of decreasing spectral amplitude with increasing source-receiver distance. The fluctuation of amplitudes evident in the figure may be caused by minor coupling differences between the geophone and the borehole wall, by shot coupling variations, and by interference effects. The low spectral amplitudes at around 50Hz are the result of recording through a notch filter.

B. The Trace Spectra of Hole Y

The spectra for traces 1 to 20 are give in Figure 5. Amplitude normalisation factors for each trace appear to the right of the diagram. As in hole W, spectrum number 1 (bottom) is computed from trace number 1

(the deepest geophone level). This spectrum looks strange compared to the other traces because this shot was a misfire and the spectrum is that of the background noise. This shot was then repeated twice after raising the shot point by 2 metres. We observe that spectra numbers 2 and 3 are almost identical, confirming that the shot is fairly repeatable, at least over this frequency range.

Spectra number 5 to 20 were obtained from another shot position located in the mudpit. These spectra are dominated by frequencies around 30 to 40Hz which signify the existence of the bubble-type pulse mentioned earlier. As in hole W, a notch filter of 50Hz has been applied to reject the power line interference. The effect can be seen on the spectra with a "hole" at 50Hz.

IV. ATTENUATION ANALYSIS BASED ON MAGNITUDE DECAY

Attenuation is usually defined to include all types of frequency selective process which contribute to the amplitude decay of propagating waves (Spencer et al., 1982). Therefore, the change of spectral magnitude with distance at each frequency component, provides a means for measuring attenuation. The process can be summarised as follows:

1. Window the data in the time domain.
2. Band-pass filtering.
3. Separation of the upgoing and downgoing waves.
4. Isolation of the first arrival downgoing waves.
5. Computation of spectral magnitudes.
6. Statistical treatment for determination of Q.

Steps 1 and 2 are an essential pre-requisite for step 3. Digital filtering not only improves the coherency of the seismic record but secures the f - k spectrum free from spatial aliasing. The band-pass filter employed by us is a box-car window convolved with a Gaussian which produces a smooth taper and minimum side-lobe effect. The bandwidth is chosen as wide as possible in order to avoid damage to the first arrival downgoing wave.

A. Method of Analysis

The spectral magnitude of the isolated first arrival DGW is computed by the Fast Fourier transform method for each level of the receiver. Ignoring source

HOLE-W: TRACE SPECTRA

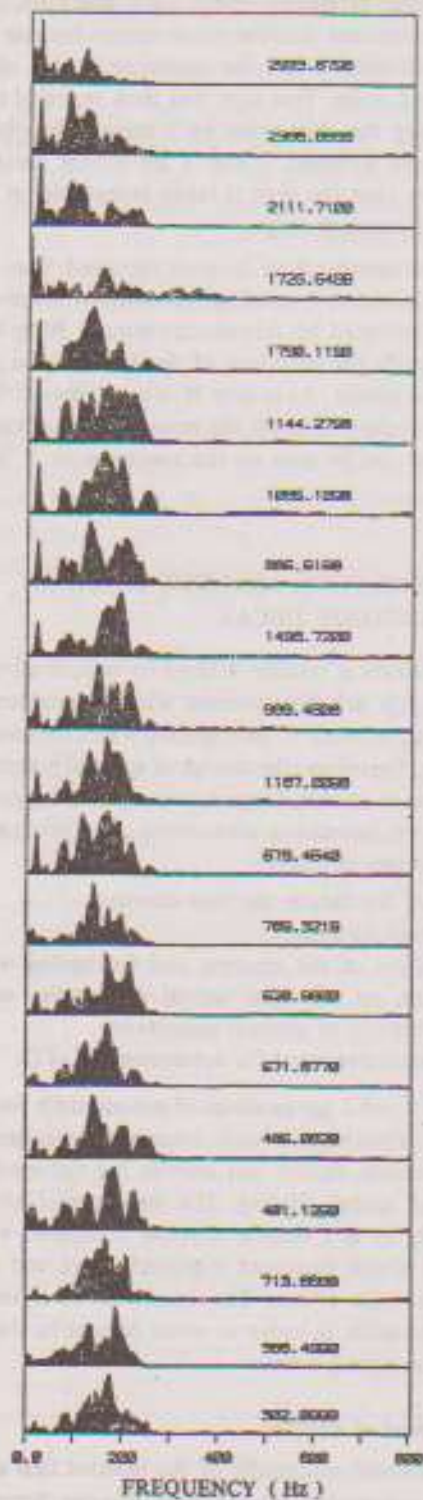


Figure 4 The spectra for hole W, traces 1 to 20 (counted from the bottom).

HOLE-Y: TRACE SPECTRA

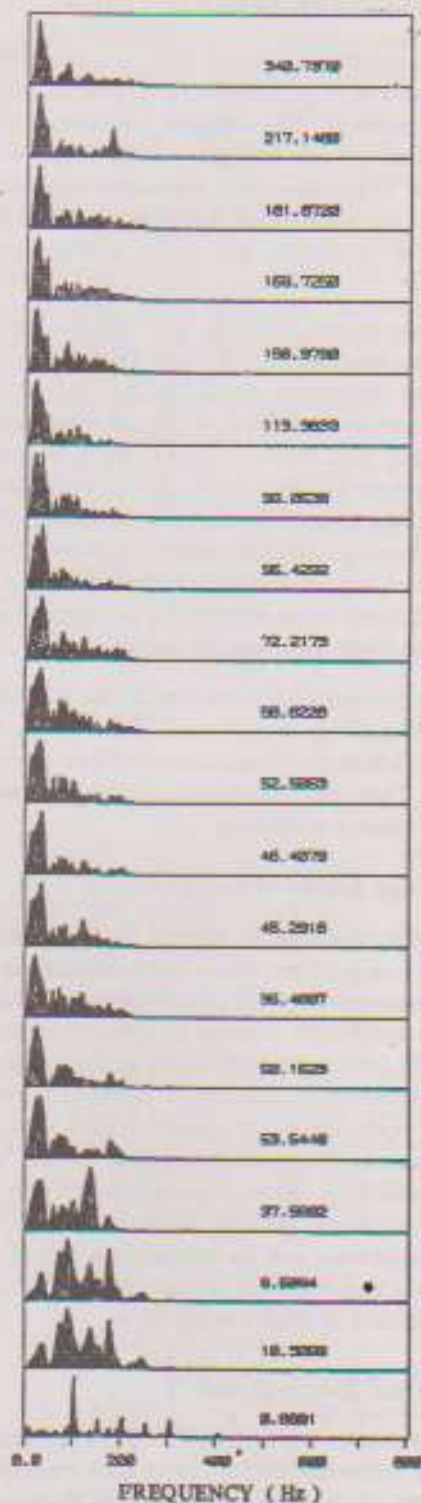


Figure 5 The spectra for hole Y, traces 1 to 20 (counted from the bottom).

and geophone coupling differences, the amplitude at frequency f and depth x can be written as

$$A(f, x) = A_0 x^{-n} e^{-\alpha(f)x} \quad (1)$$

Where n is the geometric spreading factor and $\alpha(f)$ is the attenuation coefficient. The factor n lies in the range $\frac{1}{2}$ to 2. For spherical spreading in a uniform medium n is equal to one.

After compensation for spreading and taking logarithms, we obtain the following equation for the corrected spectral amplitude

$$\ln A'(f, x) = \ln A_0 - \alpha(f)x \quad (2)$$

where $A'(f, x) = x^n A(f, x)$.

Thus for a given frequency f , the attenuation coefficient $\alpha(f)$ is determined as the slope of the $(x, \ln A')$ graph. It is preferable when carrying out the regression analysis to work with weighted spectral averages. This provides protection against small errors in the raw spectral estimates (Schoenberger and Leven, 1973; Buchanan et al., 1983). Our spectral averaging is carried out symmetrically over five neighbouring values.

The analysis is carried out for each frequency component and α , together with its standard error are computed. The whole process can be repeated for various values of n and the resulting statistics compared.

B. The Isolation of the First Arrival Downgoing Wave

A seismic trace recorded at a certain depth in a borehole contains the direct transmitted wave plus all possible upward and downward reflected waves (primaries and multiples). In attenuation analysis it is necessary to isolate the direct transmitted wave free of interference from other waves. Near-surface reverberations and tube-waves are two types of noise which often dominate the VSP record. These waves have amplitude decay characteristics which are different to that of the body waves (Hardage, 1981; Lee and Balch, 1983). Scattered waves are also present on a VSP record and they may interfere with the direct transmitted wave. If scattering occurs attenuation will be strongly frequency dependent. In this case attenua-

tion is reported to be proportional to the fourth power of frequency (Busby and Richardson, 1957; Johnston et al., 1979).

The first step in the isolation of the direct transmitted wave is the separation of downgoing waves (DGW) from upgoing waves (UGW). For this separation we employ the technique of "contour-slice filtering" (Suprajitno and Greenhalgh, 1985) which gives an excellent performance in isolating the DGW. The attraction of this process is that its pass band-stop band does not greatly perturb the natural state properties of the f - k spectrum.

For isolating the first event from other arrivals in the DGW, a time-shifted Gaussian window is used. The centre of the Gaussian function can be shifted to where the maximum of the DGW is found. Normally the maximum amplitude of each trace corresponds to the first arrival DGW. The slope of the Gaussian window should be fairly gentle and selected in full consideration of the width of the window. A narrow window may damage the pulse broadening and should be avoided. On the other hand, a wide window will admit reverberations and internal multiples, which will corrupt the attenuation estimate. A compromise must be reached after preliminary experimentation.

C. Attenuation measurement using Magnitude Decay Method

The isolated first arrival DGW of selected traces from hole W and hole Y are shown in Figure 6 and Figure 7. The spectral magnitude decay is measured from these early arrivals using the procedure outlined in section 4.2.

Figure 8 shows a representative $\ln A(f)$ versus distance from trace 1-15 of hole W at a frequency of 100Hz. A similar plot for traces 4-18 of hole Y (frequency 140Hz) is given in Figure 9. The slopes of each graph signify the attenuation coefficient. The analysis is repeated at various spectral components to yield a curve of attenuation coefficient, $\alpha(f)$ as a function of frequency.

Figure 10 is the $\alpha(f)$ for hole W which suggests a constant $Q = 20$ (velocity = 2900m/s; from f - k spectra). Figure 11 is $\alpha(f)$ for hole Y which also suggests a constant $Q = 60$ (velocity = 2800m/s. These Q values compare favourably with values of 30 and 40 obtained for British and German coal measures by

HOLE-W, TRACE 1-15. ISOLATED 1ST ARRIVALS DGW

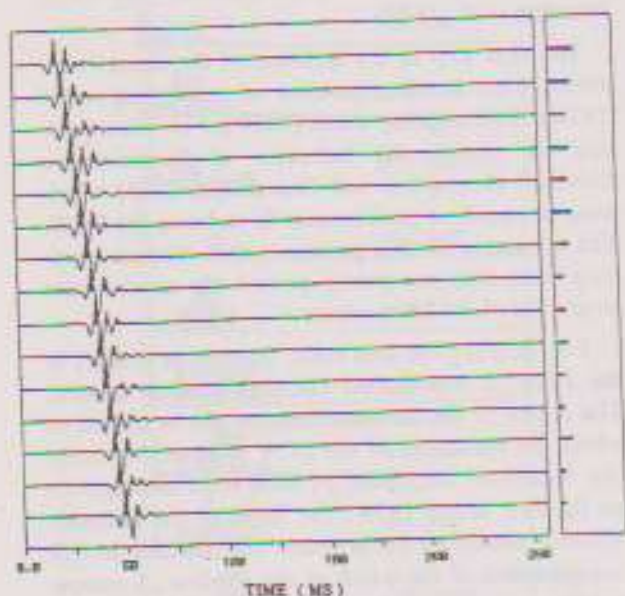


Figure 6 The isolated first arrivals downgoing waves of hole W. Pre-filtering 60-240 Hz, $\alpha = 50$. Histogram shown on the right represents the maximum amplitude of each trace relative to the others.

HOLE-Y, TR 4-18. ISOLATED 1ST ARRIVAL DGW

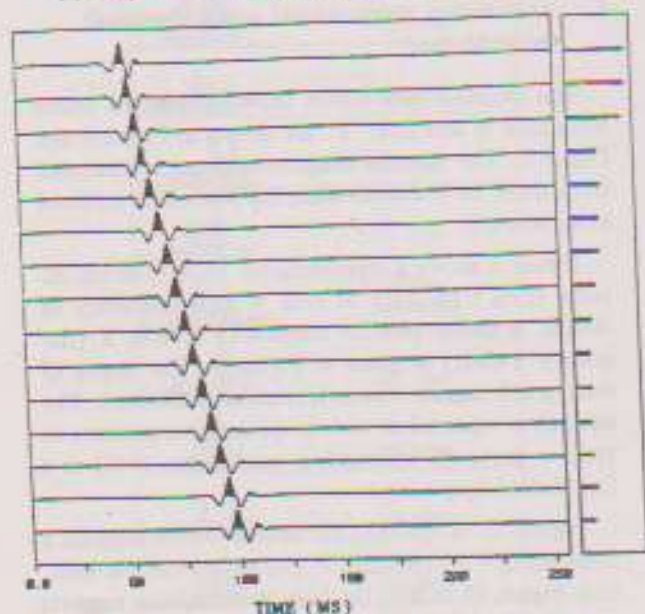


Figure 7 The isolated first arrivals downgoing waves of hole Y. Pre-filtering 60-180 Hz, $\alpha = 50$. Histogram shown on the right, represents the maximum amplitude of each trace relative to the others.

Buchanan et al. (1983) and Krey et al. (1982) respectively. The linearity of $\alpha(t)$ agrees with previous measurements (Lomnitz, 1957, 1962; Futterman, 1962; White, 1965; Kudo and Shima, 1970).

V. ATTENUATION ANALYSIS BASED ON PULSE BROADENING

A. Principle

There are numerous theories describing the effect of dissipation in shaping the seismic wavelet (e.g. Ricker, 1977). Kjartansson (1979) classified these as either constant Q theories or nearly constant Q theories, with pulse broadening a feature of both.

The measurement of pulse broadening can be done, for example, by measuring the pulse rise time or the time interval between the first inflection point and the first peak (Kjartansson, 1979). Since the rise time, τ , is related to the quality factor or dissipation factor Q (Gladwin and Stacey, 1974), the broadening of the pulse is directly related to attenuation.

Gladwin and Stacey (1974) established from field measurements the following relationship between pulse rise time τ and Q.

$$\tau = \tau_0 + \frac{Ct}{Q} \quad (3)$$

Where τ_0 indicates the rise time of the source
 C is a constant = 0.53 ± 0.04
 t is the travel time of the pulse.

The rise time is defined as the maximum amplitude divided by the maximum slope on the first break seismogram. In other words, the rise time (figure 12) can be computed from the amplitude of the first peak divided by the slope of the first inflection point (Hatherly, 1983). The quality factor Q can be extracted from the rise time-arrival time plot (equation 3) by a method of least squares.

B. The First Kick and the Point of Inflection

The first kick, which is considered to be the true arrival time of the pulse, is chosen to represent the travel time t in equation (3). To identify the first kick among the background noise we used an automated first break analysis (Suprajitno, 1986).

HOLE-W, TRACE: 1-14. AMPLITUDE DECAY AT: 120 HZ

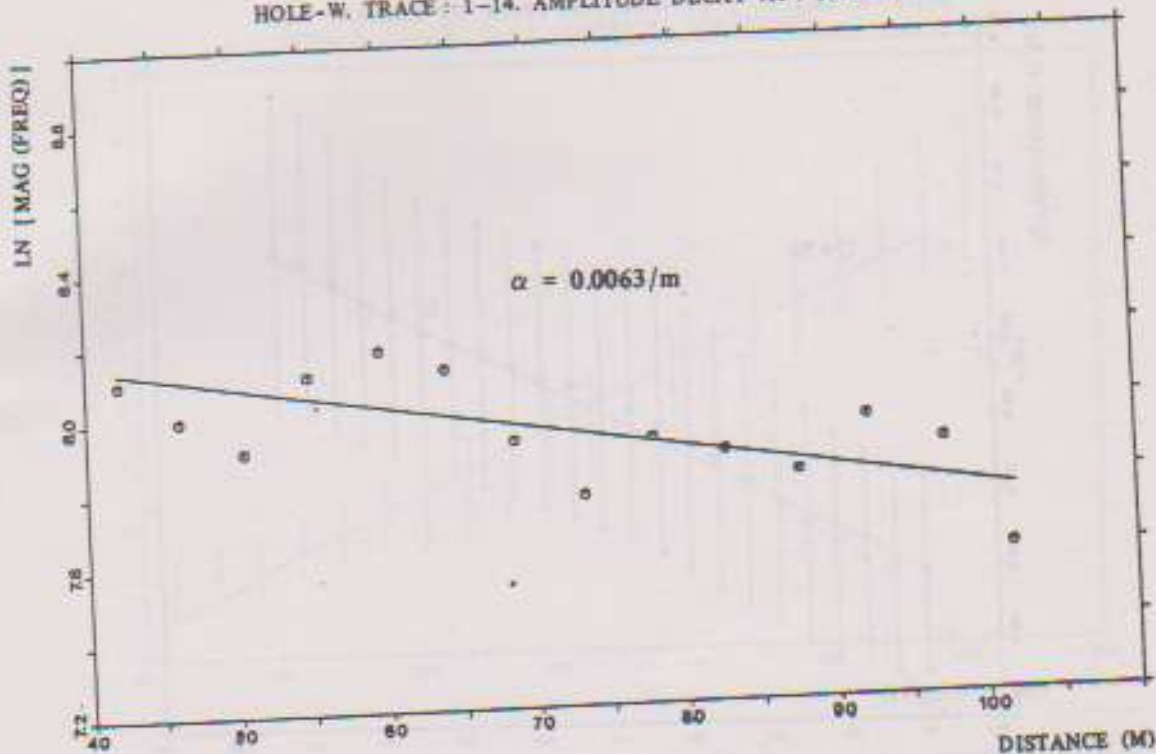


Figure 8 Attenuation diagram showing amplitude vs. distance for the 120 Hz spectral component of the isolated first arrivals downgoing waves of hole W.

The point of inflection of a signal is found if its first derivative is maximum or its second derivative equal to zero. The position of the first inflection point on the flanks of the first arrival signal can be determined rapidly and accurately using a numerical differentiation method based on the Lagrangian central difference formula. For this purpose, five pivotal points have been used in a "moving strip" mode. The formula for the second derivative is given by (Vichnevetsky, 1981, p. 64)

$$\left[\frac{\partial^2 y}{\partial t^2} \right]_n = \frac{(-y_{n-2} + 16y_{n-1} - 30y_n + 16y_{n+1} - y_{n+2})}{12 \cdot \Delta t^2}$$

Because the moving strip mode is applied over digital data, it is possible that the inflection point falls between two samples and locating this point based on the zero value of the second derivative is

HOLE-Y, TRACE: 4-18. AMPLITUDE DECAY AT: 140 HZ

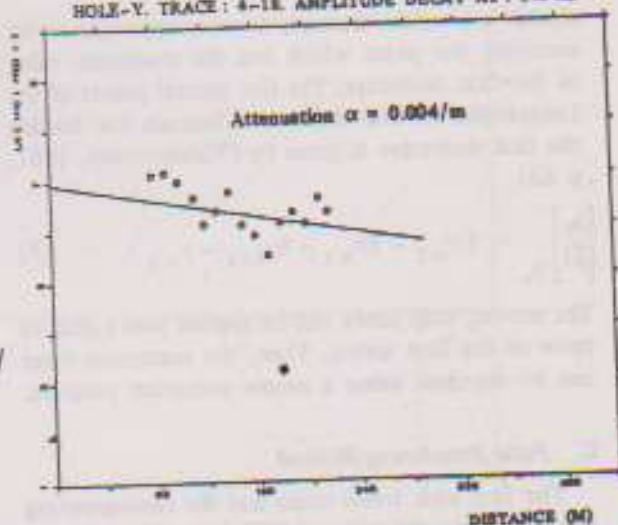


Figure 9 Attenuation diagram showing amplitude vs. distance for the 140 Hz spectral component of the isolated first arrivals downgoing waves of hole Y. Linear regression analysis yields a value of $\alpha = 0.004/m$.

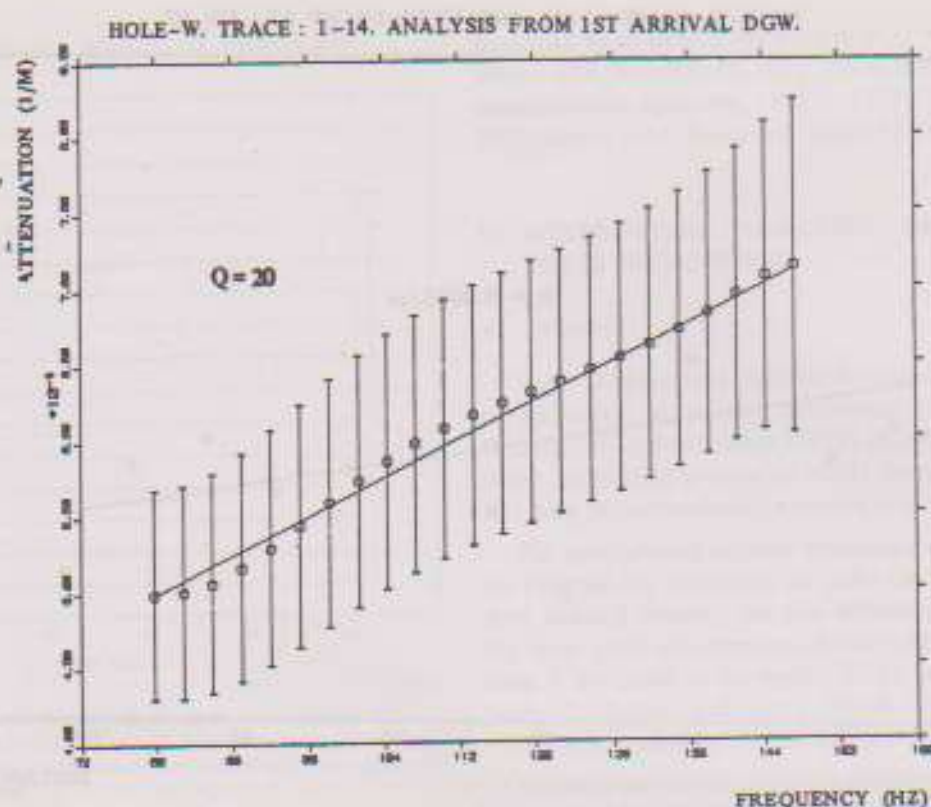


Figure 10 The attenuation coefficient vs. frequency of hole W. An approximate linear relation can be fitted implying a near-constant Q value of 20.

almost impossible. Instead, we may approximate by searching the point which has the maximum value of the first derivative. The five pivotal points of the Lagrangian central difference formula for finding the first derivative is given by (Vichnevetsky, 1981, p. 63)

$$\left[\frac{\partial y}{\partial t} \right]_n = (y_{n-2} - 8y_{n-1} - 8y_{n+1} - y_{n+2}) \quad (5)$$

The moving strip mode can be applied over a quarter cycle of the first arrival. Then, the maximum value can be searched using a simple computer program.

C. Pulse Broadening Method

The first kick travel times and the corresponding rise time from the selected VSP data of hole W and hole Y are plotted in Figure 13 and Figure 14 respectively. Linear regression analysis of the hole W data yields a constant Q value of 30 ± 2.5 (the correla-

tion coefficient is 0.76). For hole Y the results is $Q = 70 \pm 4.5$ (the correlation coefficient is 0.86).

The Q values obtained above are in close agreement with the independently determined spectral magnitude values given in section C. The discrepancy can probably be attributed to reflection/transmission losses which are incorporated into the spectral method estimates.

VI. SUMMARY

The spectral display reveals the combined effect of at least three different factors, viz. progressive earth filtering effect along the borehole, source variation, and heterogeneity of well-geophone coupling. The new processing, analysis and modelling techniques outlined earlier have been successfully applied to this field data.

The time domain attenuation analysis is straight

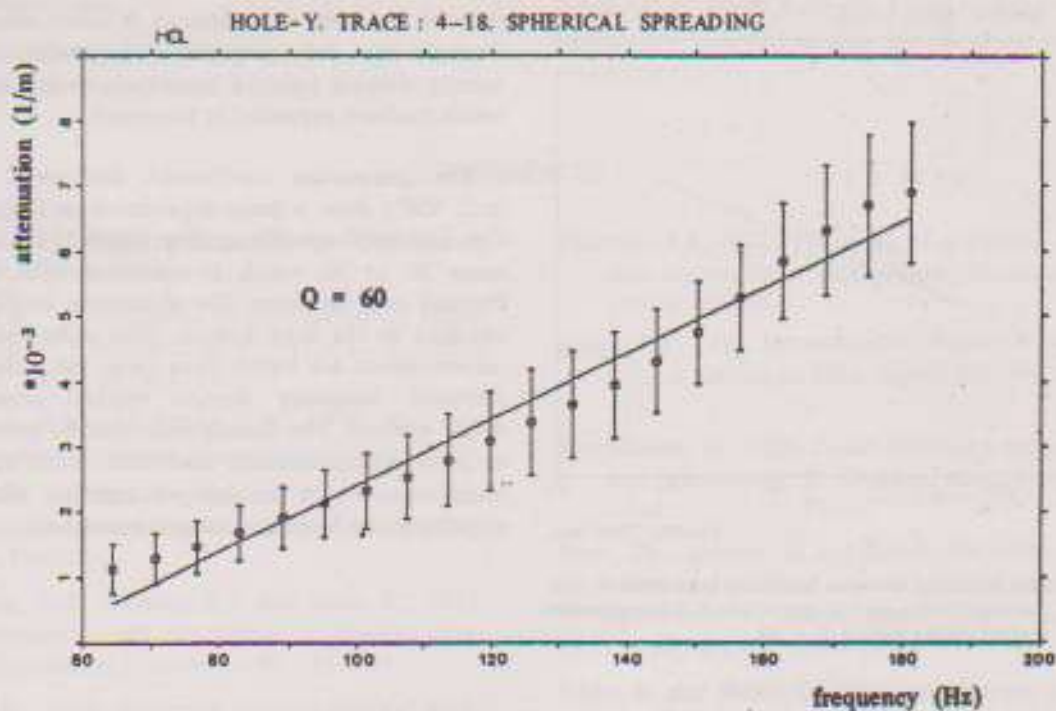


Figure 11 The attenuation coefficient vs. frequency of hole Y. An approximate linear relation can be fitted implying a near-constant Q value of 60.

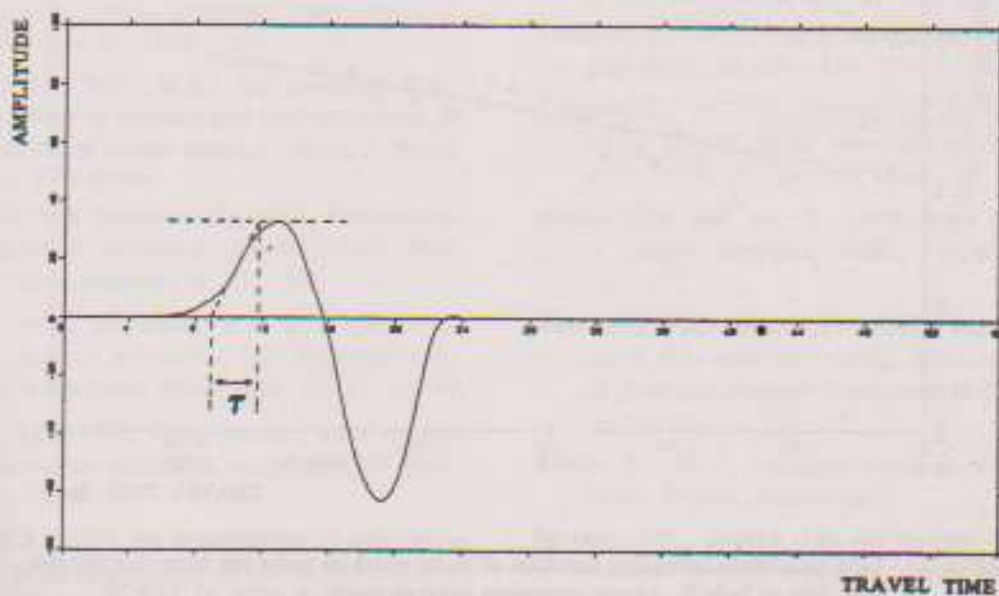


Figure 12 Pulse rise time, τ (after Hatherly, 1983).

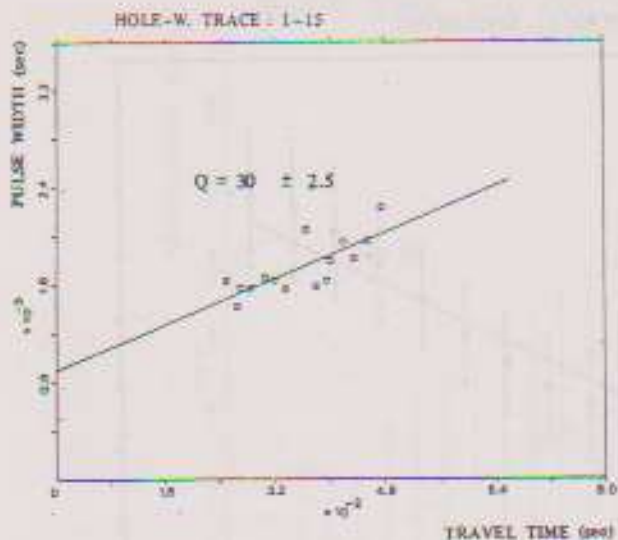


Figure 13 First kick travel times as a function of pulse width or pulse rise times for the raw VSP data of hole W. Linear regression analysis yields a value of $Q = 30$.

forward and easy to implement. It offers several advantages over and complements the traditional frequency domain (spectral magnitude decay) method which has been expanded in this paper.

The attenuation coefficients determined from both VSP's show a linear dependence on frequency. The associated specific quality factor Q lies in the range 20 to 70, which is consistent with shallow Permian coal measures. The absorption coefficients obtained in the time domain from pulse rise time measurements are higher than those using the conventional frequency domain spectral magnitude decay method. The discrepancies can be attributed to reflection/transmission coefficient losses at layer boundaries, which are lumped together with absorption in the frequency domain estimates.

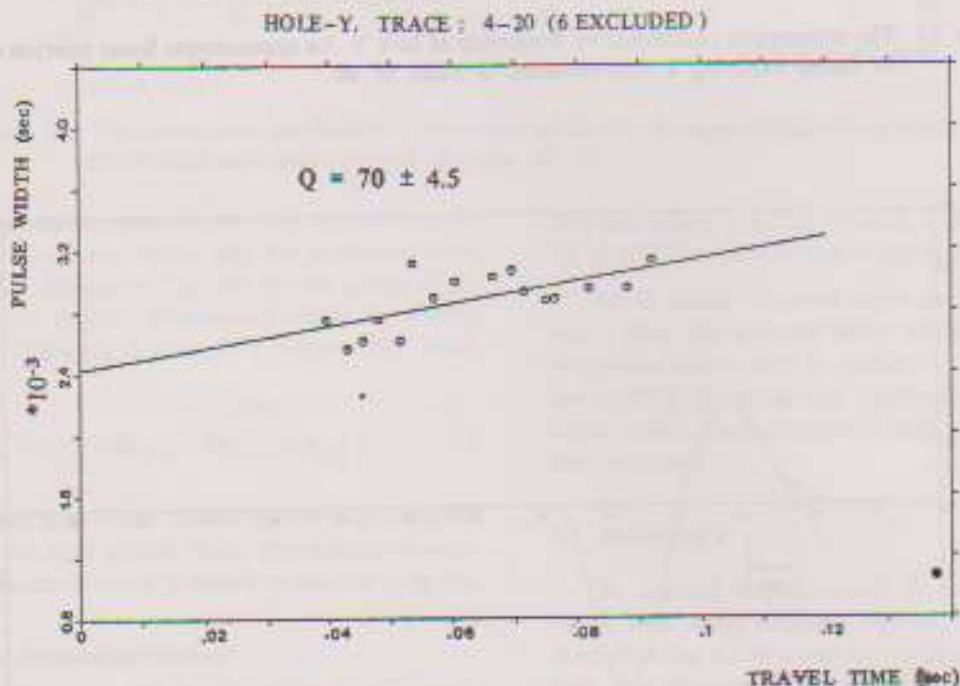


Figure 14 First kick travel times as a function of pulse width or pulse rise times for the raw VSP data of hole Y. Linear regression analysis yields a value of $Q = 70$.

Acknowledgements

The work reported in this paper is part of my research work while I was a student at the Flinders

University of South Australia. I wish to thank my supervisor Dr. S.A. Greenhalgh for his advice and encouragement.

REFERENCES

- Bath, M., 1974, *Spectral Analysis in Geophysics*, Elsevier, New York.
- Biot, M.A., 1956, Theory of propagation of elastic waves in a fluid-saturated porous solid, *J. Acous. Soc. Amer.*, 28, 168-191.
- Blackman, R.B. and Tukey, J.W., 1959, *The measurement of power spectra*, Dover, New York.
- Box, G.E. and Jenkins, G.M., 1976, *Time Series Analysis: Forecasting and Control*, Holden-Day, San Francisco.
- Buchanan, D.J., Jackson, P.J. and Davis, R., 1983, Attenuation and anisotropy of channel waves in Coal Seams, *Geophysics* 48, 133-147.
- Burg, J.P., 1967, *Maximum entropy spectral analysis*, Presented at the 37th Annual International SEG Meeting, October 31, Oklahoma.
- Busby, J. and Richardson, E.G., 1957, The absorption of Sound in sediments, *Geophysics*, 22, 281-288.
- Futterman, W.I., 1962, Dispersive body waves, *J. Geophys. Res.* 67, 5279-5291.
- Gardner, G.H.F., Willy, M.R.J. and Droschak, D.M., 1964, Effect of pressure and fluid saturation on attenuation of elastic waves in sands, *J. Petrol. Tech.*, 189-1980.
- Gladwin, M. and Stacey, F.D., 1974, Anelastic degradation of acoustical pulses in rock, *Phys. Earth Planet. Interiors*, 8, 332-336.
- Gutowski, P.R., Robinson, E.A. and Treitel, S., 1978, Spectral estimation: fact or fiction, *IEEE Trans. Geoscience Electronics*, GE-16 80-84.
- Hamilton, E.L., 1972, Compressional wave attenuation in marine sediments, *Geophysics*, 37, 620-646.
- Hardage, B.A., 1981, An examination of tube waves noise in vertical seismic profiling data, *Geophysics*, 48, 829-903.
- Hatherly, P.J., 1983, *The Analysis of shallow Refraction Seismograms*, Ph.D. Thesis, Macquarie University, Sydney.
- Hauge, P.S., 1981, Measurements of attenuation from vertical seismic profiles, *Geophysics*, 46, 1548-1558.
- Kjartansson, E., 1979, Constant Q-wave propagation and attenuation, *J. Geophys. Res.*, 84, 4737-4748.
- Krey, Th., Arnetzl, H. and Knecht, M., 1982, Theoretical and practical aspects of absorption in the application of in-seam seismic coal exploration, *Geophysics*, 47, 1645-1656.
- Kudo, K. and Shima, E., 1970, Attenuation of shear waves in soil, *Earthquake Res. Inst. Bull.*, 48, 145-158.
- Lacoss, R.T., 1971, Data adaptive spectral analysis methods, *Geophysics*, 36, 661-675.
- Lee, M.W. and Balch, A.H., 1983, Computer processing of VSP data, *Geophysics*, 48, 272-287.
- Lomnitz, C., 1957, Linear dissipation in solids, *J. App. Phys.*, 28, 201-205.
- Lomnitz, C., 1962, Application of the logarithmic creep law to stress wave attenuation in the solid earth, *J. Geophys. Res.*, 67, 365-367.
- Mavko, G.M. and Nur, A., 1978, Wave attenuation in partly saturated rocks, *Geophysics*, 44, 161-178.
- McDonald, F.J., Angona, F.A., Mills, R.L., van Nostrand, R.G. and White, J.E., 1958, Attenuation of shear and compressional waves in Pierre shale, *Geophysics*, 23, 421-439.
- Ricker, N., 1977, *Transient Waves in Visco-Elastic Media*, Elsevier, Amsterdam.
- Spencer, T.W., Sonnad, J.R. and Buttler, T.M., 1982, Seismic Q - stratigraphy or dissipation, *Geophysics*, 47, 16-24.

- Suprajitno, M., 1986, Velocity analysis of VSP data, Scientific Contribution, LEMIGAS, 2, 3-15.
- Suprajitno, M. and Greenhalgh, S.A., 1985, Separation of upgoing and downgoing waves in VSP by contour-slice filtering, *Geophysics*, 50, 950-962.
- Toksoz, M.N. and Johnston, D.H., (Eds.), 1981, *Seismic Wave Attenuation*, Geophysics reprint series, No. 2, Society of Exploration, Geophisicts, Tulsa.
- Toksoz, M.N. and Johnston, D.H. and Timur, A., 1979, Attenuation of seismic waves in dry and saturated rocks: I, Laboratory measurements, *Geophysics*, 44, 681-690.
- Treitel, S., Shanks, J.L. and Frasier, C.W., 1977, Some aspects of fan-filtering, *Geophysics*, 32, 789-800.
- Tullis, N.F. and Reid, A.C., 1969, Seismic attenuation of Gulf Coast sediments, *Geophysics*, 34, 516-528.
- Vichnevetsky, R., 1981, Computer Methods for Partial Differential Equations, Vol. 1, Prentice-Hall Inc., Englewood Cliffs, New Jersey.
- White, J.E., 1965, *Seismic Waves*, McGraw Hill, New York.
- White J.E., 1975, Computed seismic speeds and attenuation in rocks with partial gas saturation, *Geophysics*, 40, 224-232.